Exergoeconomic analysis and optimization of reverse osmosis desalination integrated with geothermal energy

Siamak Hoseinzadeh[1], Roya Yargholi[2], Hamed Kariman[2] and P. Stephan Heyns[1]

[1] Centre for Asset Integrity Management, Department of Mechanical and Aeronautical Engineering, University of Pretoria, Pretoria, South Africa

[2] Faculty of Mechanical and Energy Engineering, Shahid Beheshti University, Tehran, Iran

*Correspondence to Siamak Hoseinzadeh, Centre for Asset Integrity Management, Department of Mechanical and Aeronautical Engineering, University of Pretoria, Pretoria, South Africa.
Email: hoseinzadeh.siamak@gmail.com; Hosseinzadeh.siamak@up.ac.za

Abstract

In this research, the integrated carbon dioxide power cycle with the geothermal energy source to supply the required reverse osmosis desalination power for freshwater production is defined. The cycling power is consumed by the desalination system and sodium hypochlorite generator. Exergoeconomic analysis, and optimization are studied. Exergoeconomic analysis is shown that the desalination system, sodium hypochlorite generator, carbon dioxide turbine, and natural gas turbine have the highest rate for the sum of capital gain and exergy destruction cost. For the first case of optimization, the total cost rate is considered as the objective function. The optimal inlet discharge rate of sodium hypochlorite generator was 62% of the brine water outlet discharge rate of the desalination system. Plus, the total cost rate is reduced by 10% compared to the general case when 100% of brine water discharge rate of the desalination system enters into the sodium hypochlorite generator. The second case is multiobjective optimization to reduce costs and increase productivity.

Keywords: CO_2 power cycle; exergoeconomic; optimization; reverse osmosis desalination; sodium hypochlorite generator

1. INTRODUCTION

As it is clear, one of the crises facing humanity to survive is the scarcity of fresh water for consumption. We know that more than two-thirds of the earth is made up of water, but unfortunately 94% of it is ocean and seawater that is salty and unpalatable. Only 3% of all water in the world is usable, often found in polar glaciers and terrestrial springs. As we have learned, the high potential of salt water in the world has made people think about sweetening this water and turning it into potable water.[1-3] Kariman et al. explored a new type of industrial desalination equipment. It uses electrical energy to evaporate effluents and is environmentally friendly because of reclaimed wastewater. In this study, energy analysis was performed for the first time to identify important energy consuming equipment. Exergy analysis of the system showed that the most exergy destruction occurred in the boiler chamber and the central heat exchanger.[4] They also studied different types of desalination systems and their governing equations, then modeled the energy consumption of the evaporation vacuum evaporation system with a brine tank and reported on the economic analysis results.[5-13] Ghaebi et al. investigated the thermodynamic modeling (including energy and exergy analysis) and the exogeochemical study of a power and hydrogen generation system including an organic Rankine cycle and a proton exchange membrane electrolyzer driven by

geothermal energy, with different operating fluids (R245fa, R114, R600, and R236fa) to compare their effects on the performance of the payment system and used EES software for this purpose. Their results showed that the operating fluid R245fa has the highest energy and exergy efficiency, which are 3.11% and 67.58%, respectively. This fluid also has the highest cost savings, which is $11.54 and $4.921 per Gj for electricity and hydrogen, respectively.[14] Fontina Petrakopoulou et al. have investigated common exergy analysis and advanced exergy analysis for a hybrid power plant.[15] Galindo et al. performed an advanced exergy analysis using an experimental data set for an organic Rankine cycle coupled with an internal combustion engine. Their results show that although exergy analysis shows that exergy and boiler destruction rates are greater than expander, condenser, and pump, but advanced exergy analysis shows that expander, pump, condenser, and finally boiler are at the priority to improve equipment.[16] Sohani et al. developed a model to determine the air properties of a product of indirect dew point cooler with cross-flow heat exchanger and optimized it with neural network methods.[17, 18] They also investigated direct and indirect two-stage evaporative coolers and evaluated the impact of changes in parameters affecting different system performance criteria, including the output air conditions of each stage, cooling capacity, resource consumption and their ratio, and operating and initial costs.[19, 20] Conducted an economic analysis of the diverse water conditions and electricity conditions around the world. It was found that when the air-to-inlet ratio of the second stage is increased, there is an equality of performance criteria, so it has an optimal value.[21, 22] Also A. Abdalisousan et al. come up with a particle swarm in a new possible way. Optimization (PSO) was investigated to achieve economic optimization and in this study, the economic analysis of combined cycle power plants was performed using classical optimization. Then, external and economic algorithms and the effects of using three methods were compared and the analysis showed that the total cost of production in the unit of production is 2%, 3%, and 5% lower.[23, 24]

2. DESCRIPTION OF THE SYSTEM

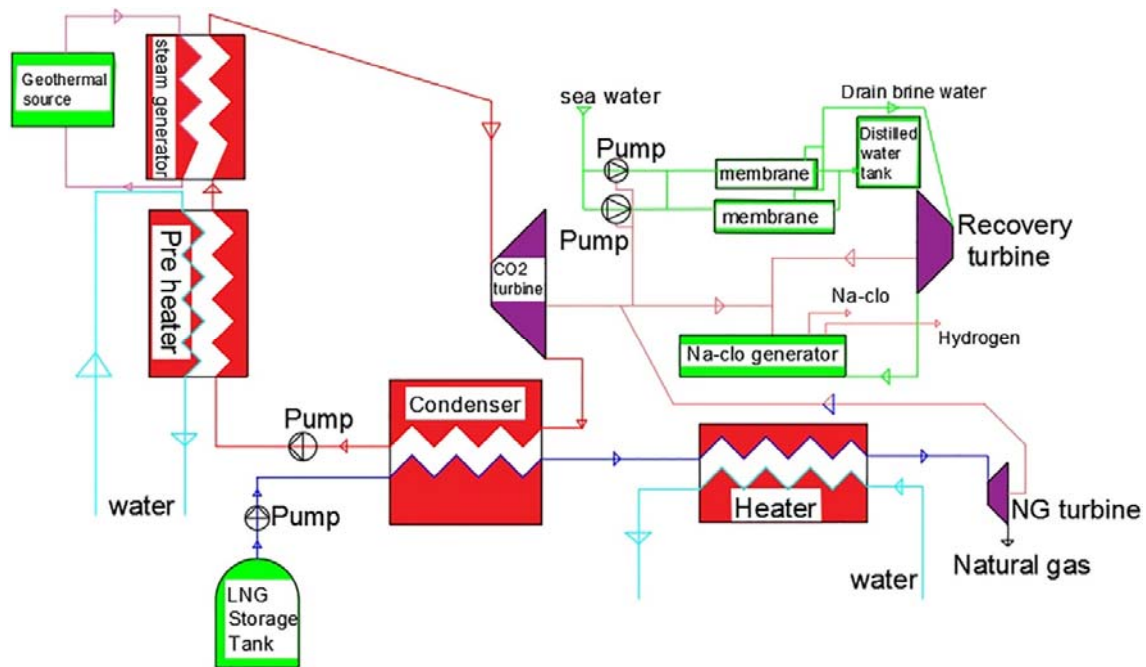Figure 1 provides a view of the model investigated in this study.

Figure 1.A view of the model presented and investigated in this study

The model consists of geothermal energy sources, complexes of power generation, drinking water production, and sodium hypochlorite production. In the carbon dioxide generation cycle, the operating fluid in the steam generator receives its required heat from the geo-thermal energy source. So reaches its supercritical state and, after generating power in the carbon dioxide turbine of this cycle, is condensed inside the condenser to enter the pump with the saturated liquid state. In order to absorb more heat from the steam generator, carbon dioxide enters the preheater before reaching the steam generator and after passing the pump to enter the steam generator at a higher temperature. In the preheater, water enters the heat exchanger at an inlet temperature equal to the ambient temperature. Since the carbon dioxide is at a temperature below zero, the water gives its heat to the carbon dioxide and cools itself. Thus, the operating fluid of this cycle enters the steam generator at a higher temperature. Now because carbon dioxide is condensed at a temperature lower than the ambient temperature, it needs a cold source or another fluid at a lower temperature. Low-temperature LNG can be used as this cold source. Therefore, the operating fluid of LNG is pumped to the condenser in the carbon dioxide cycle in the LNG gasification complex, to absorb heat and condense carbon dioxide. The LNG operating fluid, passing through this complex, completes the gasification process and the output of the complex is natural gas. Its turbine is also used to generate power. So ultimately, by using this set of processes, the heat is released from the carbon dioxide cycle, and the power is generated in its turbine. Also, the gasification of the LNG is performed. In this model, all the net power generated by the turbines is converted into electrical power by the generators. The power generated is distributed with a specific ratio between reverse osmosis desalination and sodium hypochlorite generator. Depending on the power produced in the model and the amount of it is allocated to the desalination system. The inlet discharge of the desalination system and consequently, the number of pressure chambers will be determined. As mentioned before, the inputs of the sodium hypochlorite generator are concentrated brine solution and electrical power. On the other hand, the discharge output is the concentrated brine solution; this flow is considered as the input of the sodium hypo-chlorite system. So the power required by this generator is supplied from the power output of the model. Also, the discharge flow of the desalination system has a high pressure which is equivalent to the pressure of the pumps minus the pressure drop in the complex. Therefore, this flow passes through the recovery turbine before it reaches the sodium hypochlorite generator and generates power. The generator also converts this power to electrical power and distributed along with the carbon dioxide power and LNG for use in the model.

As mentioned, the inlet flow rate of the desalination system in this model is determined according to its input power. The input power of the sodium hypochlorite generator is also determined in terms of the discharge and its inlet flow concentration. The recovery turbine power generation is also dependent on the flow passing through it. The inlet flow discharge of the sodium hypochlorite generator and the discharge flow through the recovery turbine are also dependent on the discharge feeding flow of the desalination system. Thus, the percentage of desalination power consumption relative to generated power is dependent on the discharge of sodium hypochlorite generator, or desalination output. Therefore, the total product generated in this model is entirely dependent on the total net power generated by the CO_2 and natural gas turbines.

3. EXERGOECONOMIC ANALYSIS

Exergoeconomic analysis is a combination of exergy analysis and economic concepts to provide a set of useful information on the cost of each flow necessary for optimal system design.

The modeling of the system and the exergy equations is fully described in Reference [25]. For an economic review of the process, the capital cost is calculated for all components of the model. Equations (1) to (5) present the equations used to calculate the capital cost of the various components in the process.[26]

$$C_{HX} = 130 \times \left(\frac{A_{HX}}{0.093}\right)^{0.78} \tag{1}$$

$$\log C_{Turb} = 2.6259 + 1.4398 \log(W) - 0.1776(\log(W))^2 \tag{2}$$

$$\log C_{Pump} = 3.3892 + 0.0536 \log(W_{Pump}) + 0.1538(\log(W_{Pump}))^2 \tag{3}$$

$$C_{Generator} = 60 \times (\eta_{Gen} W_{mech,in})^{0.95} \tag{4}$$

$$C_{NaClO\ Gen} = \left(\frac{W_{elec,in}}{10}\right)^{0.8} \times \frac{30000}{3.5} \tag{5}$$

Equation (1) is used to calculate the capital cost of all the heat exchangers in the model, where A_{HX} represents the area of the heat exchanger.

It is essential to use the concept of fuel and product to perform exergoeconomic analysis. For a control volume, fuel is the source of the exergy to produce the product and differs from that of real fuel such as natural gas, and so forth. The product is also the desired result produced by the fuel. Using the concepts mentioned above, the balance of exergoeconomic cost for each control volume (or component) can be in the form of Equation (6).

Table 1 shows the exogeoeconomic balance for each process component along with the auxiliary equations.

$$\dot{C}^Q + \sum \dot{C}_{in} + \dot{Z} = \dot{C}^W + \sum \dot{C}_{out} \tag{6}$$

In Equation (6) and the relationships in Tables 1-4, $\dot{Z}$ is the investment cost rate and is calculated according to the relationship (7).

$$\dot{Z} = \frac{Z.CRF.\varphi}{H} \tag{7}$$

where Z is the capital cost calculated in Equations (1) to (6). Also H is the sum of the annual working hours and is estimated to be 7,440 hours. Also φ is the maintenance factor and its value is 1.06. CRF is also the capital recovery factor and is calculated from Equation (8).

$$CRF = \frac{i(1+i)^N}{(1+i)^N - 1} \tag{8}$$

In the above relationship, i represents the interest rate and its value is 10%. N is also the lifetime, with a value of 20 years.

Table 1. Exergoeconomic balance for process components

Equipment	Exergoeconomic balance	Auxiliary equations
Steam generator	$\dot{C}_6 + \dot{C}_3 + \dot{Z}_{VG} = \dot{C}_4 + \dot{C}_7$	$\dfrac{\dot{C}_6}{Ex_6} = \dfrac{\dot{C}_7}{Ex_7}$ $\dot{C}_6 = known$
CO$_2$ turbine	$\dot{C}_4 + \dot{Z}_{Turb,CO2} = \dot{C}_5 + \dot{C}_{W,Turb,CO2}$	$\dfrac{\dot{C}_4}{Ex_4} = \dfrac{\dot{C}_5}{Ex_5}$
Condenser	$\dot{C}_5 + \dot{C}_{L2} + \dot{Z}_{condenser} = \dot{C}_1 + \dot{C}_{L3}$	$\dfrac{\dot{C}_1}{Ex_1} = \dfrac{\dot{C}_5}{Ex_5}$
CO$_2$ pump	$\dot{C}_1 + \dot{C}_{W,Pump,CO2} + \dot{Z}_{Pump,Co2} = \dot{C}_2$	$\dfrac{\dot{C}_{W,Pump,CO2}}{W_{Pump,CO2}} = \dfrac{\dot{C}_{W,Turb,CO2}}{W_{Turb,CO2}}$
Preheater	$\dot{C}_2 + \dot{C}_{S1} + \dot{Z}_{Preheater} = \dot{C}_3 + \dot{C}_{S2}$	$\dfrac{\dot{C}_2}{Ex_2} = \dfrac{\dot{C}_3}{Ex_3}$ $\dot{C}_{S1} = known$
LNG pump	$\dot{C}_{L1} + \dot{C}_{W,Pump < LNG} + \dot{Z}_{Pump,LNG} = \dot{C}_{L2}$	$\dfrac{\dot{C}_{W,Pump,LNG}}{W_{Pump,LNG}} = \dfrac{\dot{C}_{W,Pump,CO2}}{W_{Pump,CO2}}$ $\dot{C}_{L1} = known$
Heater	$\dot{C}_{L3} + \dot{C}_{S3} + \dot{Z}_{Heater} = \dot{C}_{S4} + \dot{C}_{L4}$	$\dfrac{\dot{C}_{L3}}{Ex_{L3}} = \dfrac{\dot{C}_{L4}}{Ex_{L4}}$ $\dot{C}_{S3} = known$
NG turbine	$\dot{C}_{L4} + \dot{Z}_{Turb,NG} = \dot{C}_{L5} + \dot{C}_{w,Turb,NG}$	$\dfrac{\dot{C}_{L5}}{Ex_{L5}} = \dfrac{\dot{C}_{L4}}{Ex_{L4}}$
Recovery turbine	$\dot{C}_{R2} + \dot{z}_{Rec\ Turb} = \dot{C}_{R3} + \dot{C}_{W,Rec\ Turb}$	$\dfrac{\dot{C}_{R2}}{Ex_{R2}} = \dfrac{\dot{C}_{R3}}{Ex_{R3}}$ $\dfrac{\dot{C}_{W,Rec\ Turb}}{W_{Rec\ Turb}} = \dfrac{\dot{C}_{W,Turb,CO2}}{W_{Turb,CO2}}$
Desalination	$\dot{C}_{R1} + \dot{C}_{W,in,elec,Ro} + \dot{Z}_{RO} = \dot{C}_{R2} + \dot{C}_{R4}$	$\dfrac{\dot{C}_{W,in,elec,Ro}}{W_{in,elec,Ro}} = \dfrac{\dot{C}_{W,elec,out,gen,CO2}}{W_{elec,out,gen,CO2}}$ $\dot{C}_{R1} = known$
NaClO generator	$\dot{C}_{R3} + \dot{C}_{W,in,NaClO\ gen} + \dot{Z}_{NaClO\ gen} = \dot{C}_{H2} + \dot{C}_{NaClO}$	$\dfrac{\dot{C}_{H2}}{Ex_{H2}} = \dfrac{\dot{C}_{NaClO}}{Ex_{NaClO}}$ $\dfrac{\dot{C}_{W,in,elec,Ro}}{W_{in,elec,Ro}} = \dfrac{\dot{C}_{W,in,NaClO\ gen}}{W_{in,NaClO\ gen}}$
CO$_2$ generator	$\dot{C}_{W,Turb\ CO2} + \dot{Z}_{Gen,CO2} = \dot{C}_{W,elec,out,gen,CO2}$	-
LNG generator	$\dot{C}_{W,Turb\ NG} + \dot{Z}_{Gen,NG} = \dot{C}_{W,elec,out,gen,NG}$	-
Recovery generator	$\dot{C}_{W,Rec\ Turb} + \dot{Z}_{Gen,Rec} = \dot{C}_{W,elec,out,gen,Rec}$	-

In Table 4, the values of $\dot{C}$ are unknown and their number is 32. There are also 32 unknowns in this table. Thus the basis of Table 4 is a system with 32 equations and 32 unknowns. It is possible to solve such systems in different software using coding (including MATLAB software).

For comparison from the perspective of exergoeconomic analysis, several parameters have been defined. Three parameters of this type have been defined in Equations (9) to (11).

$$r_k = \frac{c_{P,k} - c_{F,k}}{c_{F,k}}$$

(9)

$$\dot{C}_{D,k} = c_{F,k} \dot{Ex}_k^D$$

(10)

$$f_k = \frac{\dot{Z}_k}{\dot{Z}_k + \dot{C}_{D,k}}$$

(11)

In Equation (9), r_k is the relative cost difference for the kth component. This parameter indicates the difference between the average cost of products and fuel due to the destruction and cost of investment. In this relationship, $c_{P,k}$ and $c_{F,k}$ are respectively the average cost per unit exergy of product and fuel for the component k, and their values are obtained from Equations (12) and (13).

$$c_{P,k} = \frac{\dot{C}_{P,k}}{\dot{Ex}_{P,k}}$$

(12)

$$c_{F,k} = \frac{\dot{C}_{F,k}}{\dot{Ex}_{F,k}}$$

(13)

In Equation (10), $\dot{C}_{D,k}$ is equivalent to the exergy destruction cost in the kth component.

In Equation (11), f_k is the exergoeconomic factor.

Table 2 has provided the product cost of each component $(\dot{C}_{P,k})$ and the fuel cost of each component $(\dot{C}_{F,k})$ in Equations (12) and (13), for example, for any type of equipment used in the process.

Table 2. Product cost and fuel cost of some model equipment

Equipment	Fuel cost	Product cost
Steam generator	$\dot{C}_{F,VG} = \dot{C}_6 - \dot{C}_7$	$\dot{C}_{P,VG} = \dot{C}_4 - \dot{C}_3 = \dot{C}_{F,VG} + \dot{Z}_{VG}$
CO_2 turbine	$\dot{C}_{F,Turb,CO2} = \dot{C}_4 - \dot{C}_5$	$\dot{C}_{P,Turb,CO2} = \dot{C}_{W,Turb\,CO2}$
CO_2 pump	$\dot{C}_{F,Pump,CO2} = \dot{C}_{W,Pump,CO2}$	$\dot{C}_{P,Pump,CO2} = \dot{C}_1 - \dot{C}_2$
CO_2 generator	$\dot{C}_{F,Gen\,Co2} = \dot{C}_{W,Turb\,CO2}$	$\dot{C}_{P,Gen\,Co2} = \dot{C}_{W,elec,uotlet,Gen\,CO2}$

Also, the product cost rate is obtained from the exergoeconomic perspective for the whole process from the Equation (14).

$$\sum \dot{C}_P = \sum \dot{C}_F + Z \tag{14}$$

4. OPTIMIZATION

As described in previous sections, the discharge water output from the desalination system has higher concentration than the feed water of the system which is seawater and if it is discharged into the environment or into free waters, it can cause pollution and be harmful. Therefore, in this model, this highly brine water stream was used as the sodium hypochlorite generator input. But on the other hand, the usual discharge of this salty stream into the sea does not require much cost and power unless it incurs a large fine.

Therefore, the question here is about the effectiveness of desalination discharge flow as a sodium hypochlorite generator input and its production in terms of economy and exergy. More precisely, what percentage of this saline discharge stream enters the sodium hypochlorite generator to minimize the total cost rate of the process, calculated from Equation (14).

Optimization using single-objective genetic algorithm by MATLAB software has been used in this study. In this optimization, the permissible range of decision-making parameter, which is equal to the ratio of inlet discharge flow of sodium hypochlorite generator to discharge rate of outlet brine flow of desalination, is considered from 0 % to 100%. Also, a multi-objective optimization is performed by MATLAB to reduce the cost rate and increase the efficiency by the multi-objective genetic algorithm method. Multi-objective genetic algorithm is one of the multi-objective evolutionary algorithms and uses random and repetitive search to find optimal results. Figure 2 provides an illustration of the performance of multi-objective evolutionary algorithms.[26]
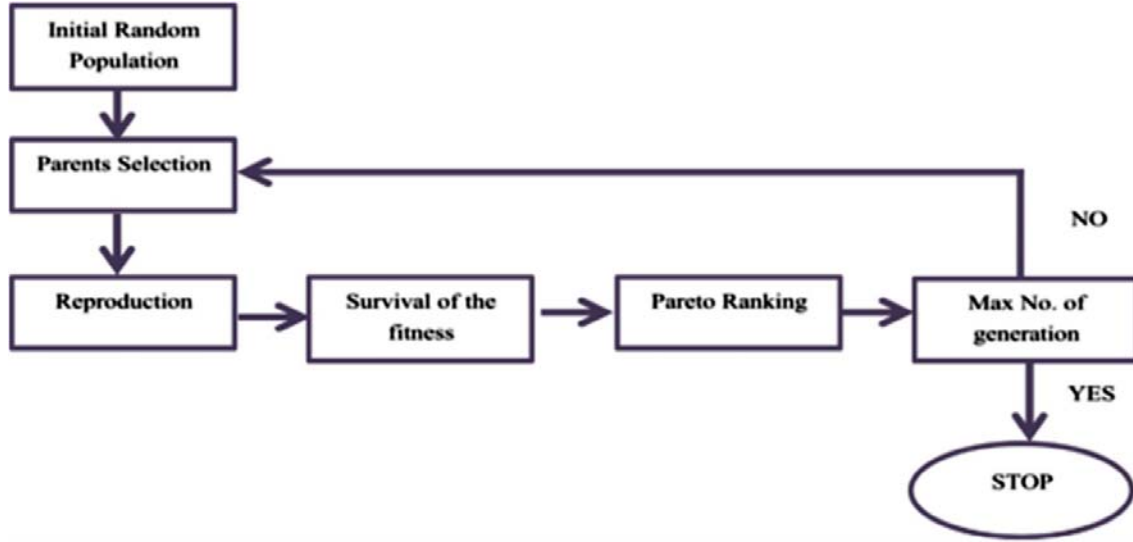
Figure 2. Graph of multi-objective optimization algorithm

In this optimization it is attempted to have the lowest cost rate parameter of the whole process, obtained from Equation (14), and also to achieve the highest efficiency of this process.

A number of parameters can be considered to consider the efficiency of the process, including the amount of potable water produced along with the amount of sodium hypochlorite produced in the process, or the total power or net power produced in the process. But it should be noted that all of these values are strongly interdependent. So if it gets the maximum amount of net power generated by carbon dioxide turbine and natural gas turbine, then it will definitely have the highest amount of potable water and sodium hypochlorite production. And as a result, it will also have the highest power output from the recovery turbine.

In this optimization, the sum of net power of carbon dioxide and LNG flow has been considered as the second objective function and is obtained from Equation (15).

$$W_{Net,cycles} = W_{Net,LNG} + W_{Net,CO2} \tag{15}$$

This optimization has three decision parameters. These parameters are inlet temperature of carbon dioxide turbine, inlet pressure of carbon dioxide turbine, and inlet pressure of carbon dioxide pump. The range of variation of these parameters in optimization has been presented in Equations (16) and (17), respectively.

$$110 \le T_4 \le 120°C \tag{16}$$

$$11 \le P_4 \le 12 \, MP \tag{17}$$

$$0.6 \le P_1 \le 0.7 \, MP \tag{18}$$

8

4.1. The assumptions and conditions of the model for simulation

In order to model the process presented, assumptions are applied to simplify the problem. These assumptions are as follows:

- The system is examined under stable conditions.
- Heat transfer between the environment and system components is neglected.
- The pressure drop inside the transmission pipes is ignored.
- Kinetic energy and potential are neglected in all processes.
- The pressure drop in all heat exchangers is 2%.
- The carbon dioxide and LNG fluids in the proposed cycle have a saturated liquid state at the pump inlet.

For numerical modeling of the proposed system, the desalination water input conditions has been based on Bushehr city data in May 2007. Table 3 presents the modeling requirements of the desired process.

Table 3. Modeling of the desired process[25, 26]

Parameter	Value	Unit
Pressure of environment	325/101	kPa
Temperature of environment	25	°C
Temperature of geothermal water	140	°C
Pressure of geothermal water	700	kPa
Flow rate of geothermal water	10	Kg/s
Reject temperature of geothermal water	85	°C
Inlet temperature of CO_2 turbine	120	°C
Inlet pressure of CO_2 turbine	12	MPa
CO_2 turbine isentropic efficiency	70	%
Condensation temperature	−10	°C
CO_2 pump isentropic efficiency	80	%
Temperature of LNG tank	−47/161	°C
Pressure of LNG tank	43/101	kPa
Working pressure of LNG tank	3175/6	MPa
NG turbine isentropic efficiency	80	%

LNG pump isentropic efficiency	70	%
Outlet pressure of NG turbine	4	MPa
Temperatures of desalination feed water	25	°C
Pressure of distilled water	101	kPa
Recovery rate of desalination	3/0	-
Inlet pressure of desalination pump	101	kPa
Desalination pump isentropic efficiency	80	%
Recovery turbine isentropic efficiency	80	%
Outlet pressure of recovery turbine	303	kPa
Efficiency of generators	95	%
Temperature decreasing of hot section of heater and pre heater	20	°C
TDS of desalination feed water	35,612	Mg/l
Number of membrane in pressure cell	6	-

5. RESULTS

This section presents the results obtained from exergoeconomic analysis and optimization.

After performing exergoeconomic analysis, the product cost and fuel cost of each component are calculated and then we can calculate the parameters of the exergoeconomic analysis factor evaluation, the cost of exergy destruction, and the cost difference ratio. These values have been presented in Table 4.

Considering the thermoeconomic evaluation criteria for designing a thermodynamic system, a great deal of attention needs to be paid to the component that has higher sum of the capital cost rate and the cost of exergy destruction.26 According to Table 4, this sum is highest for sodium hypochlorite generator, condenser, carbon dioxide turbine, and heaters, respectively. As such, these components are of the most importance from the exergoeconomic point of view.

Preheaters, condensers, pumps in the LNG stream, carbon dioxide turbine generator, and natural gas turbine generator have the lowest exogenous factor. This indicates that the costs associated with these components are almost exclusively related to the cost of exergy destruction. Represents the relative cost difference, which is due to the investment cost and exergy destruction costs. This parameter is preferred to be low. The f and r parameters for desalination system are large. So if the capital cost for this component is reduced, its effectiveness on improving the total cost of the system will be large.

Table 4. Cost of exergy destruction and the cost difference ratio

Equipment	$c_f \left(\frac{\$}{Gj}\right)$	$c_P \left(\frac{\$}{Gj}\right)$	E_D (kW)	$\dot{C}_D \left(\frac{\$}{year}\right)$	$\dot{C}_D + \dot{Z} \left(\frac{\$}{year}\right)$	f(%)	r(%)
Steam generator	1.3000	4.7147	355.4500	14,570	18,288	20.3154	262.6681
CO_2 turbine	9.4197	16.2593	343.7200	102,110	127,950	20.1966	72.6095
Condenser	4.2211	9.4197	952.8800	126,840	133,960	5.3142	123.1596
CO_2 pump	16.2593	23.1554	23.3400	11,970	13,659	12.3643	42.6580
LNG pump	16.2593	77.5605	76.8300	39,400	41,241	4.4706	377.0210
Heater	12.2920	94.3479	262.5100	101,760	109,630	7.1777	667.5543
NG turbine	12.2920	18.1988	58.4200	22,650	36,965	38.7333	48.0538
CO_2 turbine generator	16.2593	17.2981	25.3600	13,010	13,475	3.4845	6.3889
NG turbine generator	18.1988	19.2739	5.0100	2,880	2,977	3.3797	5.9077
NaClO generator	20.1300	80.7603	404.1700	256,580	287,080	10.6233	301.1927
Desalination	20.2277	55.4625	18.2800	11,670	60,196	80.6188	174.1906
Recovery turbine	12.3189	16.2593	2.4500	880	3,257	73.0838	43.6477
Recover turbine generator	16.2593	18.8245	1.0400	540	690	22.3706	15.7763

5.1. Presentation of optimization results

According to the results obtained in the previous sections, the power consumption of sodium hypochlorite is higher than the desalination power consumption and also higher exergy destruction cost, its input value can be controlled. Considering the reduction in total cost rate as the objective function and the percentage of desalination discharge water that enters the sodium hypochlorite generator as the decision parameter in a single-objective optimization, the sodium hypochlorite generator discharge rate for the optimal state will be 62% of the outlet discharge rate of brine water of the desalination system. The total cost rate before this optimization is 145,470 \$/year and after that optimization is 130,360 \$/year. Therefore, this optimization reduces the total cost rate by 10%.

The second optimization is a two-objective optimization with objective functions of total cost rate and total net power generated from carbon dioxide cycle and LNG flow. The goal is to minimize total cost and maximize net power generation. Increasing the net power output in this model also results in increased freshwater production and also the sodium hypochlorite generator. The results of this optimization have been presented in 20 different cases in Table 5 and Figure 3, which represent the Pareto diagram of this optimization.

Table 5. Results of this optimization

| Number	Inlet pressure of CO_2 turbine (MPa)	Inlet pressure of CO_2 pump (MPa)	Inlet temperature of CO_2 turbine (C^0)	Total cost of process ($/year)	Total net power of cycle and CO_2 flow-LNG flow
1	11.8110798	0.604011552	119.6672018	147,575.0247	611.4507084
2	11.02586087	0.699992064	110.0217366	137,808.7869	563.0301265
3	11.2672631	0.689368291	113.5622965	138,631.5162	569.0757018
4	11.81099294	0.607557963	119.6073147	144,278.9217	599.0470679
5	11.10823697	0.6950417	112.0661194	138,467.1151	566.2258633
6	11.80856718	0.603454007	119.5365632	144,905.742	600.6060897
7	11.62981671	0.6285758	117.5649917	143,194.6303	590.9523677
8	11.51073546	0.651923919	116.3817073	141,055.7948	582.347159
9	11.56807786	0.605124389	119.2770789	147,256.6291	608.5099878
10	11.52254721	0.619475557	119.2692882	145,726.4002	602.7989893
11	11.8092709	0.603499118	119.609092	144,901.4465	600.5375943
12	11.7505139	0.616833846	117.9810988	144,064.4472	595.9211149
13	11.34502457	0.68844744	113.4226069	138,679.0185	569.5874246
14	11.69146324	0.614647174	119.4389093	146,584.6867	606.2489511
15	11.6108931	0.623819317	117.6794614	143,296.8331	592.3684098
16	11.797511	0.684930816	117.1138825	139,425.7187	573.8768919
17	11.8110798	0.604011552	119.6672018	147,575.0247	611.4507084
18	11.48705974	0.675312949	114.217334	140,027.1951	574.2820515
19	11.63372296	0.639562128	117.5806167	142,409.065	587.1240213
20	11.10848111	0.697971388	112.0504944	137,894.4344	565.3707203
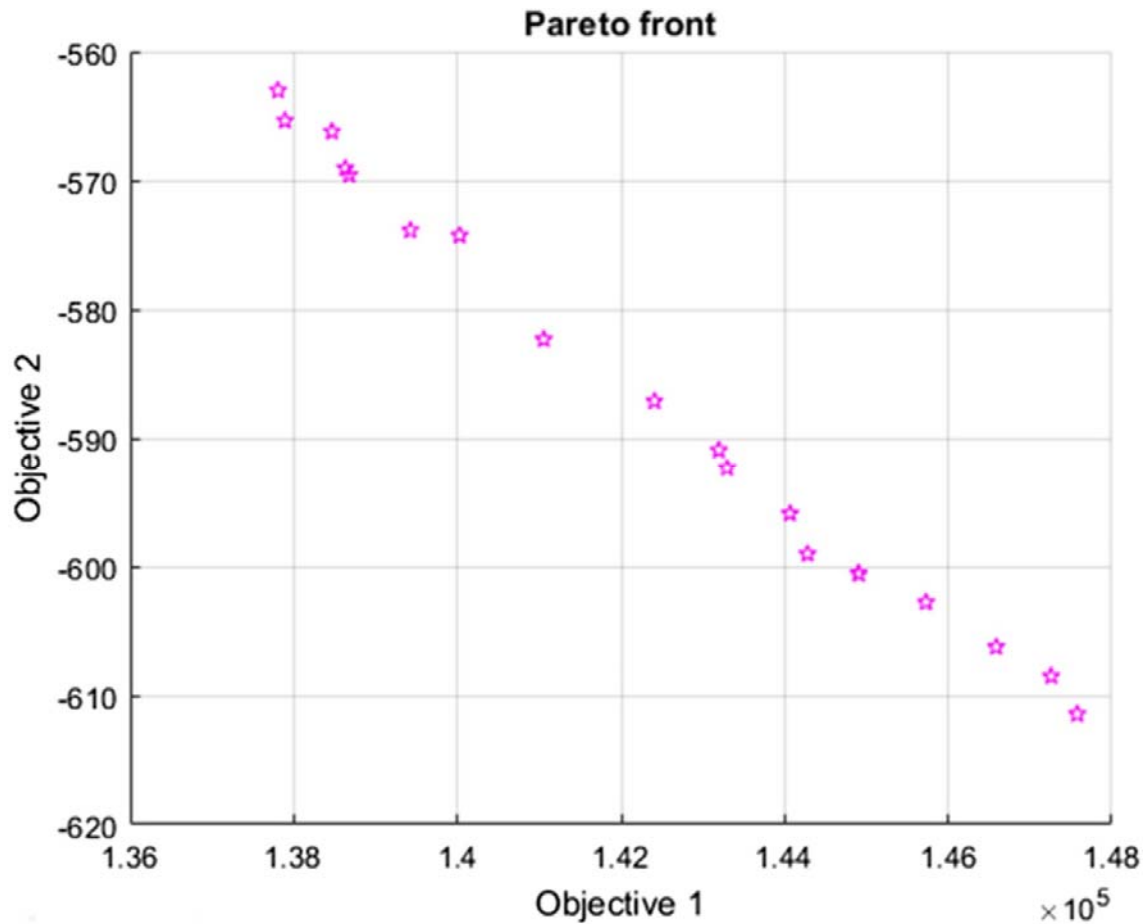
Figure 3. Pareto diagram of two-objective optimization

Figure 3 has presented the numbers corresponding to the net power generation with negative sign. The reason for this is that for multi-objective optimization by genetic algorithm based on MATLAB software, the goal of optimization is to minimize all input objective functions. Consequently, when the goal is to maximize the parameter as the objective function, this parameter must be entered negatively into the algorithm. Therefore, in these results, we consider the absolute values of the values shown in the Pareto diagram.

6. CONCLUSION

In this study, exergoeconomic and optimization analyzes were performed for a model for seawater desalination and cogeneration of sodium hypochlorite. The power required in this model was provided by the organic carbon dioxide power cycle and the liquefied natural gas gasification cycle for the conversion of liquefied natural gas and heat capture from carbon dioxide. Geothermal energy was also used as the heat source of the carbon dioxide cycle.

In this model, the generators of sodium hypochlorite, condenser, carbon dioxide turbine, and heater generate the most cost for the system. Most of the condenser costs are related to its exergy destruction, and on the other hand, much of the exergy destruction is inevitable and cannot be recovered. It is therefore advisable to consider the other components listed above to improve costs. In this model, if we consider the cost of discharging saline water out of the freshwater into nature as negligible, by transferring 2% of this water to the sodium

hypochlorite generator and discharging the remaining 2% after passing the recovery turbine to the sea, we will have a 5% reduction in the total cost rate, which is optimal.

Nomenclature

Q
  heat transfer (kJ)

W
  mechanical power output (kJ)

H
  enthalpy (kJ/kg)

M^0
  mass flow (kg/s)

R
  global constants of gases (Lit atm/mol K^0)

T
  flow temperatures (C^0)

K_w
  water permeability coefficient

P
  pressure (MPa)

A_m
  area of membrane (m)

X
  concentration (g/L)

Ex
  exergy (kJ)

MW
  molar mass (mol)

I
  exergy destruction (kJ)

Z
  capital cost ($)

Z^0
  investment cost ($/year)

CRF

capital recovery factor

N

lifetime (year)

r_k

relative cost difference ($)

c

average cost per unit exergy ($/kJ)

C^0

exergy destruction cost ($/kJ)

f_k

exergoeconomic factor

Greek letters

η

efficiency (%)

π

osmotic pressure (atmosphere)

ρ

density (kg/m^3)

φ

maintenance factor

REFERENCES

[1]El-Dessouky H, Alatiqi I, Bingulac S, Ettouney H. Steady-state analysis of the multiple effect evaporation desalination process. *Chem Eng Technol*. 1998; 21(5): 437- 451.

[2]Ali MB, Kairouani L. Multi-objective optimization of operating parameters of a MSF-BR desalination plant using solver optimization tool of Matlab software. *Desalination*. 2016; 381: 71- 83.

[3]Malik SN, Bahri PA, Vu LT. Steady state optimization of design and operation of desalination systems using Aspen custom modeler. *Comput Chem Eng*. 2016; 91: 247- 256.

[4]Kariman H, Hoseinzadeh S, Heyns PS. Energetic and exergetic analysis of evaporation desalination system integrated with mechanical vapor recompression circulation. *Case Stud Thermal Eng*. 2019; 16:100548.

[5]Kariman H, Hoseinzadeh S, Shirkhani A, Heyns PS, Wannenburg J. Energy and economic analysis of evaporative vacuum easy desalination system with brine tank. *J Therm Anal Calorim*. 2019; 1- 10. https://doi.org/10.1007/s10973-019-08945-8.

[6]Hoseinzadeh S, Heyns PS, Chamkha AJ, Shirkhani A. Thermal analysis of porous fins enclosure with the comparison of analytical and numerical methods. *J Therm Anal Calorim*. 2019; 138: 727- 735. https://doi.org/10.1007/s10973-019-08203-x.

[7]Hoseinzadeh S, Moafi A, Shirkhani A, Chamkha AJ. Numerical validation heat transfer of rectangular cross-section porous fins. *J Thermophys Heat Transf.* 2019; 33: 698- 704. https://doi.org/10.2514/1.T5583.

[8]Yousef Nezhad ME, Hoseinzadeh S. Mathematical modelling and simulation of a solar water heater for an aviculture unit using MATLAB/SIMULINK. *J Renew Sustain Energy.* 2017; 9(6):063702. https://doi.org/10.1063/1.5010828.

[9]Hoseinzadeh S. Thermal performance of electrochromic smart window with nanocomposite structure under different climates in Iran. *Micro Nanosyst.* 2019; 11(2): 154- 164. https://doi.org/10.2174/1876402911666190218145433.

[10]Hoseinzadeh S, Hadi Zakeri M, Shirkhani A, Chamkha AJ. Analysis of energy consumption improvements of a zero-energy building in a humid mountainous area. *J Renew Sustain Energy.* 2019; 11. https://doi.org/10.1063/1.5046512.

[11]Hoseinzadeh S, Azadi R. Simulation and optimization of a solar-assisted heating and cooling system for a house in northern of Iran. *J Renew Sustain Energy.* 2017; 9:045101. https://doi.org/10.1063/1.5000288.

[12]Hoseinzadeh S, Heyns PS, Kariman H. Numerical investigation of heat transfer of laminar and turbulent pulsating Al2O3/water nanofluid flow. *Int J Numer Meth Heat Fluid Flow.* 2019; ahead-of-print.

[13]Javadi MA, Hoseinzadeh S, Khalaji M, Ghasemiasl R. Optimization and analysis of exergy, economic, and environmental of a combined cycle power plant. *Sadhana Acad Proc Eng Sci.* 2019; 44(5): 121. https://doi.org/10.1007/s12046-019-1102-4.

[14]Ghaebi H, Farhang B, Parikhani T, Rostamzadeh H. Energy, exergy and exergoeconomic analysis of a cogeneration system for power and hydrogen production purpose based on TRR method and using low grade geothermal source. *Geothermics.* 2018; 71: 132- 145.

[15]Petrakopoulou F, Tsatsaronis G, Morosuk T, Carassai A. Conventional and advanced exergetic analyses applied to a combined cycle power plant. *Energy.* 2012; 41(1): 146- 152.

[16]Galindo J, Ruiz S, Dolz V, Royo-Pascual L. Advanced exergy analysis for a bottoming organic rankine cycle coupled to an internal combustion engine. *Energy Convers Manag.* 2016; 126: 217- 227.

[17]Sohani A, Sayyaadi H, Hoseinpoori S. Modeling and multi-objective optimization of an M-cycle cross-flow indirect evaporative cooler using the GMDH type neural network. *Int J Refrig.* 2016; 69: 186- 204.

[18]Sohani A, Sayyaadi H. Thermal comfort based resources consumption and economic analysis of a two-stage direct-indirect evaporative cooler with diverse water to electricity tariff conditions. *Energy Convers Manag.* 2018; 172: 248- 264.

[19]Sohani A, Sayyaadi H. Design and retrofit optimization of the cellulose evaporative cooling pad systems at diverse climatic conditions. *Appl Therm Eng.* 2017; 123: 1396- 1418.

[20]Sohani A, Sayyaadi H, Zeraatpisheh M. Optimization strategy by a general approach to enhance improving potential of dew-point evaporative coolers. *Energy Convers Manag.* 2019; 188: 177- 213.

[21]Sohani A, Naderi S, Torabi F. Comprehensive comparative evaluation of different possible optimization scenarios for a polymer electrolyte membrane fuel cell. *Energy Convers Manag.* 2019; 191: 247- 260.

[22]Sohani A, Sayyaadi H, Balyani HH, Hoseinpoori S. A novel approach using predictive models for performance analysis of desiccant enhanced evaporative cooling systems. *Appl Therm Eng.* 2016; 107: 227- 252.

[23]Abdalisousan A, Fani M, Farhanieh B, Abbaspour M. Multi-objective thermoeconomic optimisation for combined-cycle power plant using particle swarm optimisation and compared with two approaches: an application. *Int J Exergy.* 2015; 16(4): 430- 463.

[24]Abdalisousan A, Fani M, Farhanieh B, Abbaspour M. Effect of decision variables in the steam section for the exergoeconomic analysis of TCCGT power plant: a case study. *Energy Environ*. 2014; 25(8): 1381- 1404.

[25]Naseri A, Bidi M, Ahmadi MH. Thermodynamic and exergy analysis of a hydrogen and permeate water production process by a solar-driven transcritical CO2 power cycle with liquefied natural gas heat sink. *Renew Energy*. 2017; 113: 1215- 1228.

[26]Ahmadi MH, Mehrpooya M, Pourfayaz F. Exergoeconomic analysis and multi objective optimization of performance of a carbon dioxide power cycle driven by geothermal energy with liquefied natural gas as its heat sink. *Energy Convers Manag*. 2016; 119: 422- 434.